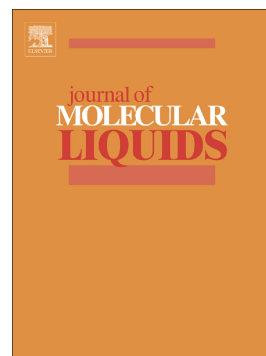


Journal Pre-proof

Multifunctional hydrogel based on ionic liquid with antibacterial performance

Yang Yu, Zeyu Yang, Shujing Ren, Yanan Gao, Liqiang Zheng



PII: S0167-7322(19)33138-1

DOI: <https://doi.org/10.1016/j.molliq.2019.112185>

Reference: MOLLIQ 112185

To appear in: *Journal of Molecular Liquids*

Received date: 3 June 2019

Revised date: 27 September 2019

Accepted date: 20 November 2019

Please cite this article as: Y. Yu, Z. Yang, S. Ren, et al., Multifunctional hydrogel based on ionic liquid with antibacterial performance, *Journal of Molecular Liquids*(2019), <https://doi.org/10.1016/j.molliq.2019.112185>

This is a PDF file of an article that has undergone enhancements after acceptance, such as the addition of a cover page and metadata, and formatting for readability, but it is not yet the definitive version of record. This version will undergo additional copyediting, typesetting and review before it is published in its final form, but we are providing this version to give early visibility of the article. Please note that, during the production process, errors may be discovered which could affect the content, and all legal disclaimers that apply to the journal pertain.

© 2019 Published by Elsevier.

Multifunctional hydrogel based on ionic liquid with antibacterial performance

Yang Yu,^a Zeyu Yang,^c Shujing Ren,^a Yanan Gao,^{*,b} and Liqiang Zheng^{*,a}

^a Key Laboratory of Colloid and Interface Chemistry, Shandong University, Ministry of Education, Jinan, 250100, China

^b Key Laboratory of Ministry of Education for Advanced Materials in Tropical Island Resources, Hainan University No 58, Renmin Avenue, Haikou, 570228, China

^c China Research Institute of Daily Chemical Industry Co., Ltd. Taiyuan, Shanxi, CN 030000

*Corresponding author: Liqiang Zheng E-mail address: lqzheng@sdu.edu.cn

Yanan Gao E-mail address: ygao@hainanu.edu.cn

Abstract

Biocompatible antibacterial hydrogels as novel dressing materials have been a widely researched method in modern medical technology. Here, we designed and prepared a new type of multifunctional antibacterial hydrogels that used poly(vinyl alcohol) (PVA)-tetrahydroxyborate anion ($\text{B}(\text{OH})_4^-$) hydrogel as a vector and pyrrolidinium ionic liquids (ILs) as antibacterial drugs. The formation of borate ester bonds between PVA and $\text{B}(\text{OH})_4^-$ as dynamic network junctions endows hydrogels with multiple functions. Moreover, the as-prepared hydrogel exhibited effective anti-microbial activity against *Escherichia coli* and *Staphylococcus aureus*. Our results indicated that the hydrogels containing ILs with longer alkyl chain exhibited more pronounced antibacterial properties.

The moisture retention, self-healing, syringeability and multiresponse behavior together with the antibacterial properties of the hydrogels make them ideal candidates as multifunctional dressing materials for joint skin wound healing.

Keywords: *Ionic liquid antibacterial hydrogels multifunctional dressing materials*

Introduction

The skin is the outermost organ of the body that protects the body from the external environment.¹ Skin wounds are susceptible to bacterial attack, thus causing infection. Bacterial infection is one of the most common clinical diseases; this type of infection can endanger human health and even threaten human life.² The ideal wound dressing would prevent the wound from being further damaged and infected and accelerate the healing process. In 1962, Dr. Winter first proposed a new concept of the moisturizing environment of the wound that contributes to wound healing. A moist wound bed prevents tissue dehydration and apoptosis and promotes angiogenesis.³ Epithelial cells are more prone to migration in humid compared with dry environments during wound healing, and the growth factors in the wound fluid are more active in the environment attached to occlusive dressing.⁴ However, traditional dressings, such as cotton wool, bandages and gauzes, provide poor occlusion and tend to promote water evaporation, resulting in a relatively open dehydrated

wound bed.^{5, 6}

Hydrogels have a 3D network structure through physical or chemical crosslinking⁷⁻⁹ that absorbs a large amount water or biological fluids, swells without structure destruction and provides a suitable 3D environment and mechanical protection.¹⁰ In addition, hydrogels have many features, such as good biocompatibility, adjustable strength and flexibility, providing a broad application prospects in the biomedical field.^{11, 12} As an improvement upon the traditional wound healing agents, antibacterial hydrogels have become a research hotspot.

As research continues to advance, many advanced antibacterial hydrogels with versatility have been developed. As an emerging category of antibacterial materials, hydrogels with unique properties, such as responsiveness^{13, 14} and self-healing, have been reported.^{15, 16} The design of multifunctional and multiresponsive smart hydrogels with self-healing and self-supporting properties in noncovalent systems has attracted particular interest due to their wide applications in biotechnology,¹⁷ adaptability and reversibility.¹⁵ Dynamic covalent chemistry is one method for the preparation of smart materials based on reversible covalent bonds, which integrate both the stability of covalent bonds and the reversibility of noncovalent bonds. Dynamic materials with controllable structure and chemical properties have broad applications in biomedical fields. The formation of borate ester by the reversible and

controllable “click reaction” between boronic acid and diol has been intensively studied and can be readily used for the construction of molecular receptors.¹⁸ Meanwhile, with the introduction of borate ester functionality, these materials exhibit attractive properties, such as glucose-sensitivity, reversibility and self-healing. These materials have a wide range of applications, especially in biomedical areas.

Poly(vinyl alcohol) (PVA) is a nontoxic, degradable and water-soluble polymer.¹ PVA-based hydrogels have exhibited many beneficial properties, such as high biocompatibility, good biodegradability and adhesion performance. $B(OH)_4^-$ interacts with two distinct *cis*-diol groups on PVA to yield the formation of a hydrogel system. Hence, antibacterial hydrogels provide versatility and responsiveness by incorporating antibiotics into PVA- $B(OH)_4^-$ hydrogels. However, the long-term use of antibiotics has led to the emergence of many drug-resistant bacteria that are very difficult to conquer.¹⁹ Moreover, conventional antibiotics are associated with numerous other problems, such as solubility, overdose, and cytotoxicity.² Therefore, it is critical to identify new types of antibacterial drug with different antimicrobial mechanisms and effective and safe drug delivery systems.

Cationic liposomes consisting of a polar head group and a hydrophobic lipid moiety exhibit definite antibacterial effects. In addition, their antibacterial mechanism is different from that of traditional antibiotics.^{20,}

²¹ Cations preferentially adsorb the negatively charged cell wall by electrostatic interactions, and hydrophobic chains are subsequently inserted into the lipophilic region of the cell membrane. Such an interaction results in physically irreparable damaged bacterial cell membranes and reduce bacterial resistance. This new antibacterial mechanism illuminates method to combat bacterial resistance.

Ionic liquids (ILs) have been known for a long time as organic salts; nevertheless, research on and the application of ILs have been decreasing. The special properties of ILs, such as high thermal stability, negligible vapor pressure, conventional nonflammability, and outstanding solvation properties,^{22, 23} make them widely used in many applications, such as catalysis, biocatalysis, synthetic chemistry and electrochemistry.^{22, 24} Their most prominent feature is the ability to regulate physicochemical properties, such as viscosity, hydrophobicity, boiling point, melting point and solubility, through proper selection of anions and cations. Previous studies have demonstrated that ILs with cations, such as ammonium, imidazolium, pyridinium, quinolinium, and phosphonium, exhibit excellent antibacterial properties.²⁵⁻²⁹

Inspired by the antibacterial mechanism of cationic liposomes, herein we designed and prepared a series of ILs based on pyrrolidinium cations with different alkyl chain lengths as antibacterial drugs. PVA-B(OH)₄⁻ hydrogel was selected as vector to make the antimicrobial hydrogel

multifunctional and expand its potential application in biomedical fields. The cross-linking mechanism of PVA-B(OH)₄⁻ is reversible and transient as well as pH and glucose sensitive resulting in the conversion between the sol-gel. The multifunctional hydrogel is expected to overcome multiple limitations of currently available antibiotics and has potential applications in antibacterial dressings and topical administration.

Experimental

Materials

Briefly, 1-methylpyrrolidine (98%, Shanghai Aladdin Chemistry Co. Ltd), 1-alkyl bromide C_nH_{2n+1}Br (98%, n=4, 6, 8 and 12, Beijing J&K Scientific, Ltd), poly(vinyl alcohol) (99% hydrolyzed, Beijing J&K Scientific, Ltd), boracic acid (AR, Shanghai Sinopharm Chemical Reagent Co. Ltd), sodium hydroxide (AR, Shanghai Sinopharm Chemical Reagent Co., Ltd), ether absolute (AR, Tianjin Tian in Fuyu Fine Chemical Co., Ltd) and ethyl acetate (AR, Tianjin Tian in Fuyu Fine Chemical Co., Ltd) were used as-purchased without further purification. Deionized water was used throughout the experiments.

Synthesis of Pyrrolidinium Ionic Liquids C_nMPBr (n=4, 6, 8 and 12)

The compound 1-methylpyrrolidine was dissolved in ethyl acetate. Then, an equimolar amount of 1-alkyl bromide C_nH_{2n+1}Br (n=4, 6, 8 and 12) in ethyl acetate was slowly added to the solution at room temperature under a nitrogen atmosphere. The reaction mixture was then stirred at

room temperature for 48h. After the reaction, the solution was filtered and the resulting residue was purified with ether absolute at least thrice. The obtained ionic liquid (IL) C_n MPBr was dried under vacuum at room temperature for 24 h, and the product was obtained. The purity of the product was ascertained by ^1H NMR (300 MHz, D_2O).

C_4 MPBr δ (relative to TMS): 3.36 (s, 4H), 3.25 – 3.13 (m, 2H), 2.89 (s, 3H), 2.07 (s, 4H), 1.73 – 1.55 (m, 2H), 1.34 – 1.18 (m, 2H), 0.81 (t, 3H).

C_6 MPBr δ (relative to TMS): 3.43 (s, 4H), 3.32 – 3.20 (m, 2H), 2.97 (s, 3H), 2.15 (s, 4H), 1.82 – 1.65 (m, 2H), 1.28 (td, $J = 9.4, 8.4, 4.5$ Hz, 6H), 0.83 (t, 3H).

C_8 MPBr δ (relative to TMS): 3.50 – 3.39 (m, 4H), 3.33 – 3.20 (t, 2H), 2.98 (s, 3H), 2.16 (s, 4H), 1.83 – 1.66 (m, 2H), 1.38 – 1.20 (m, 10H), 0.82 (t, 3H).

C_{12} MPBr δ (relative to TMS): 3.47 – 3.36 (m, 4H), 3.30 – 3.18 (m, 2H), 2.96 (s, 3H), 2.13 (s, 4H), 1.72 (s, 2H), 1.31 – 1.14 (m, 18H), 0.78 (t, 3H).

Preparation of Hydrogels

PVA was dissolved in distilled water at a concentration of 5wt% under continuous magnetic stirring for 3 hours at a temperature of 90 °C to obtain homogenous solution A. C_n MPBr was formulated into 0.5 mol/L solution B. Briefly, 0.5 mol/L $\text{NaB}(\text{OH})_4$ solution C was prepared by dissolving NaOH and H_3BO_3 . PVA/ C_n MPBr hydrogels were prepared by mixing solution A and solution B at a volume ratio of 2:1 under stirring.

The fabrication of PVA/C_nMPBr/B(OH)₄⁻ hydrogels were prepared by mixing solution A, solution B and solution C according to the volume ratio of 2:1:1 under stirring.

Characterization

Fourier transform infrared (FT-IR) spectra

After removing H₂O, hydrogels were converted to xerogel by freeze-drying under vacuum. FT-IR spectra were obtained at a resolution of 2 cm⁻¹ using a BIORADFTS-165 spectrometer.

Thermal properties

Thermogravimetric analysis (TGA) was performed on a Rheometric Scientific thermoanalyzer (Piscataway, NJ) under nitrogen flow with a 10 °C/min heating rate from room temperature to 650 °C.

Scanning electron microscopy (SEM) micrographs

A Gemini SEM 300 scanning electron microscope was used to obtain the cross-section morphology micrographs of the hydrogels at ambient temperature and low vacuum. After removing H₂O, hydrogels were converted to xerogel by freeze-drying under vacuum. The xerogel was coated with a 100-150 Å Au layer by sputtering.

Degree of swelling of membrane

The hydrogels were dried under vacuum to constant weight. Dried hydrogels were immersed in phosphate buffer saline (pH=7.4). The hydrogels were removed from solutions, wiped with tissue paper 2 to 3

times at set intervals and weighted as quickly as possible using a digital microbalance. The experiment was repeated thrice and results were averaged. The degree of swelling (DS) was calculated using the following formula:³⁰

$$W = \frac{W_1 - W_2}{W_2} \times 100\%$$

where, W_1 and W_2 are the mass of the swollen and dried hydrogels, respectively.

Rheological Measurements

Rheological measurements were obtained using a Haake RheoStress 6000 rheometer with a cone-plate system (C35/1 Ti) at 25 °C. For each sample, a dynamic frequency sweep measurement was recorded in the linear viscoelastic region, which was determined from dynamic stress sweep measurement.

Self-healing

The hydrogels (diameter 6.4 mm, thickness 3 mm) were dyed different colors (red, yellow, blue and purple), and then, the cut surfaces were brought together to make a contact at room temperature without the application of an outside stimulus. Subsequently, the healed samples were used in the self-supporting test.

Syringeability

Solution D was obtained by mixing 0.5 mol/L IL C_n MPBr solution

with an equal volume of 0.5 mol/L B(OH)_4^- solution. A 5 wt % PVA solution colored by bromothymol blue served as solution E. Solution D and E were placed in different syringes for injectable experiments.

Environmental responsiveness test

(1) pH responsiveness

Briefly, 0.5 mL of 0.1 mol/L HCl or NaOH was added to the synthesized PVA/ $\text{C}_n\text{MPBr}/\text{B(OH)}_4^-$ hydrogel to explore its pH response performance.

(2) Glucose responsiveness

Here, 0.5 mL 0.1 mol/L glucose was added to the synthesized PVA/ $\text{C}_n\text{MPBr}/\text{B(OH)}_4^-$ gel to investigate its glucose response performance.

Antibacterial Test

Antibacterial activities of the hydrogels against *Escherichia coli* (CGMCC 1.12883) and *Staphylococcus aureus* (CMCC 26003) which are the most common microorganisms found on burn wounds, were tested using the agar diffusion method to measure the zone of inhibition. The zone of inhibition was defined as the clear region around the sample disc saturated with an antimicrobial agent on the agar surface. The zone of inhibition, expressed in mm, was calculated using the following formula:

$$\text{inhibition zone(mm)} = (D - d)/2$$

where D is the diameter of the inhibition zone and d is the diameter of the sample expressed in mm.

Briefly, 1 mL of the OD₆₀₀=0.9 bacterial solution was inoculated onto 250 mL of sterilized Luria Bertani (LB) agar medium, and a sample disc with a diameter of 6.4 mm was placed on the inoculated agar plate after the medium was solidified. After 24 h incubation at 37 °C, colonies were visualized and digital images were captured. The formed clear zones diameters were measured. Each sample was repeated thrice.

Results and Discussion

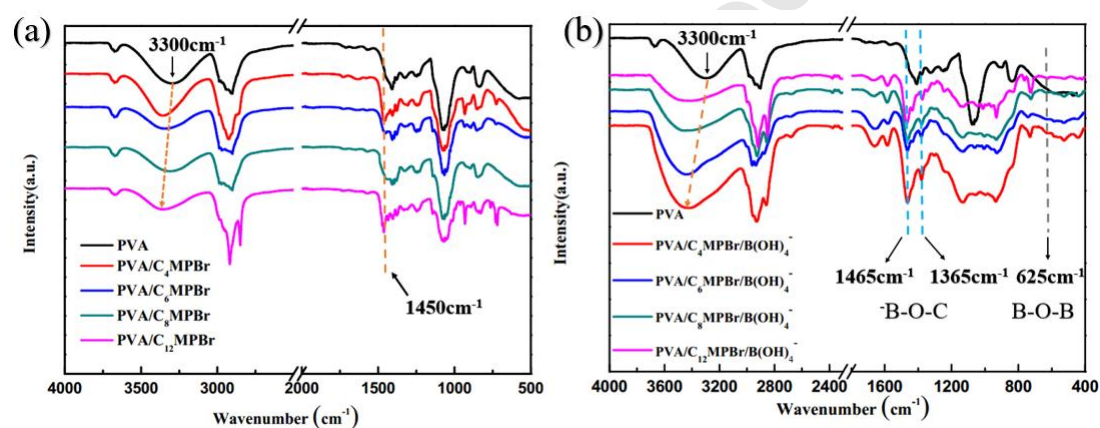


Figure 1. FTIR spectra for the (a) pure PVA and PVA/C_nMPBr and (b) PVA/C_nMPBr (n=4,6,8 and 12).

FTIR spectra of pure PVA, PVA/C_nMPBr and PVA/C_nMPBr/B(OH)₄⁻ are shown in Figure 1; these results support the interaction among components. The broad peak in the range of 3000-3600 cm⁻¹ corresponds to hydroxyl group of PVA.³¹ After the incorporation of IL into the PVA, a characteristic peak derived from the pyrrolidinium cation appeared at 1450 cm⁻¹ (Figure 1a). The peak positions and intensity of the hydroxyl group are sensitive to hydrogen bonding. The interaction between pyrrolidinium

cations and the oxygen of hydroxyl leads to partial hydrogen bond cleavage. The intensity of hydroxyl characteristic peaks decreased, and their maximum absorption wavelength shifts to a higher wavenumber due to the chaotropic effect of ILs.³² This interaction is also reflected in the appearance of the hydrogel as shown in Figure 2. PVA and IL are combined by ion-dipole interactions, which weaken the hydrogen bonding between the PVA segments, thus forming an opaque hydrogel. As shown in Figure 1b, a significant difference was observed after the addition of $B(OH)_4^-$. $B(OH)_4^-$ participates in “click reactions” with diols and their congeners with dynamic covalent functionality.³³ The dynamic crosslinking between PVA and $B(OH)_4^-$ is indicated by the characteristic peaks at 1465 and 1365 cm^{-1} (asymmetric stretching vibration of B–O–C) and 625 cm^{-1} (bending of B–O–B linkage within the borate networks),^{31, 34} indicating that the -OH groups on the PVA interact with the borate ions to form a borate bond. Borate ions connect the PVA chain segments into a 3D network structure by means of borate bonding, and IL is well dispersed in the hydrogel system by virtue of electrostatic interactions. As a result, a uniform and transparent hydrogel is obtained (Figure 2b). The 3D networks and the water absorbency of hydrogels are indispensable for the implantation of the antibacterial functions of ILs. In addition, the dynamic covalent crosslinking between PVA and $B(OH)_4^-$ forms a reversible network that endows hydrogels with new functions, such as

glucose-responsivity, reversibility, and self-healing.

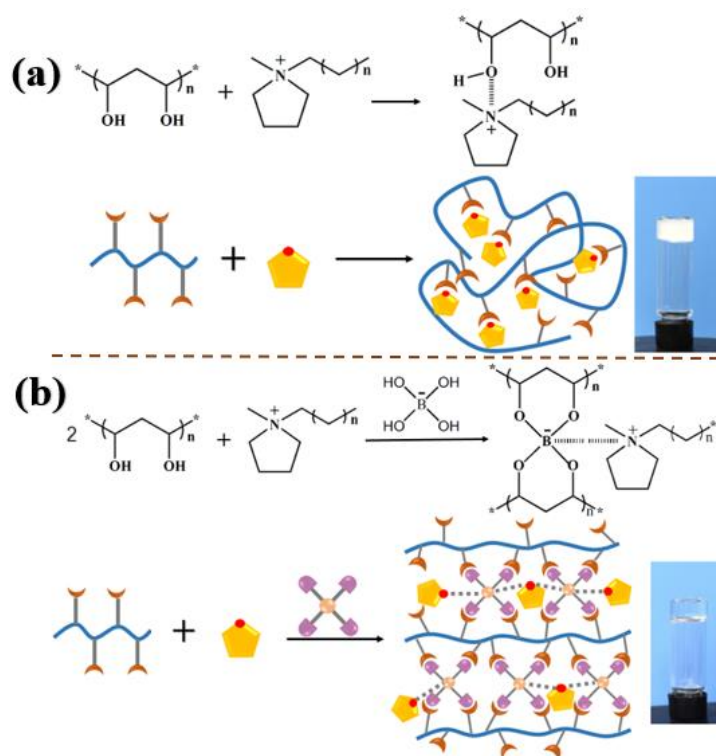


Figure 2. Formation mechanism and schematic diagram of PVA/C₄MPBr and PVA/C₄MPBr/B(OH)₄⁻ hydrogel.

The microscopic morphology of the hydrogel skeleton was observed by SEM in Figure 3. The PVA/C₄MPBr hydrogel exhibits a uniform dense structure, and no porous structure is observed, as shown in Figure 3a. After B(OH)₄⁻ was introduced into the PVA/C₄MPBr hydrogel system, the hydrogel exhibits a highly loose porous 3D network structure due to the cross-linking between PVA and B(OH)₄⁻ (Figure 3b). The porous structure is beneficial to absorb and retain moisture. This feature is in accordance with the DS measurement where the water content of these hydrogels accounts for greater than 94 wt%, revealing that the hydrogels

maintain a moist healing environment for the wound. TGA is used to measure the thermal stability of hydrogels shown in Figure S1. The pure PVA began to decompose at 220 °C while the PVA/C_nMPBr/B(OH)₄⁻ hydrogels exhibited a higher decomposition temperature at 260 °C. The increased thermal stability of the hydrogel is also due to the dense network structure.³⁵

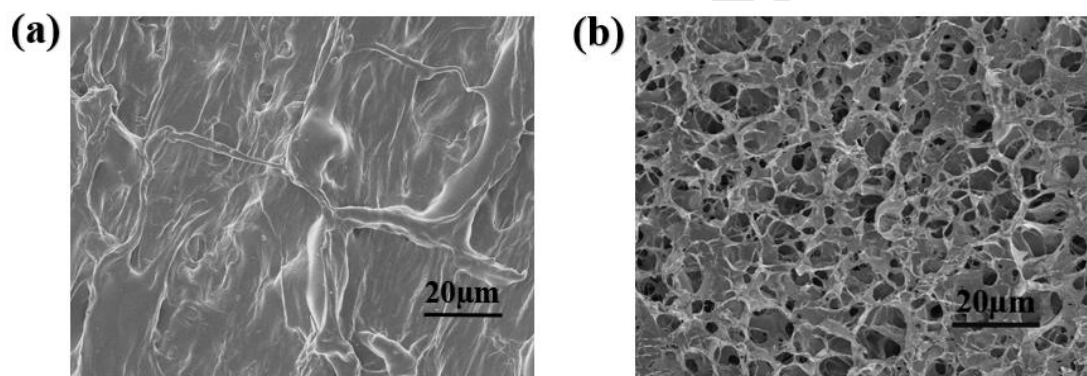


Figure 3. SEM images of hydrogels (a) PVA/C₄MPBr and (b) PVA/C₄MPBr/B(OH)₄⁻.

Recently, *in situ* formed hydrogels have been recognized for their potential biomedical applications, including minimally invasive drug delivery, injectable tissue engineering, surgical glues, tissue sealants, and adhesion prevention coating.^{36, 37} An important direction in the development of hydrogel-based technology is the preparation of injectable hydrogels under mild conditions. Gel precursors (sol) are injected to form a hydrogel through a sol-to-gel transition mechanism. To achieve *in situ* hydrogel formation, the reaction must be performed

under mild conditions with a fast reaction rate for simultaneous injection. The gelation rate of the hydrogel significantly influences its practical application.³⁸ A mixed solution of 0.5 mol/L C_nMPBr and $B(OH)_4^-$ and a pure 5 wt% PVA solution (bromothymol blue added) were prepared separately (Figure 4a-d). Of note, the gelation process can be quickly realized within 30 s when the two solutions are simultaneously extruded from the syringe. The interaction between borate and hydroxyl groups is particularly effective for the formation of 3D network structures, prompting dynamic crosslinking to occur very quickly at room temperature.³⁹ This injectable hydrogel has high plasticity, which can be adapted to the shape of various wounds. Although polymer-based gels have superior performances, their desirable properties tend to deteriorate when they are damaged by cracks on a macro or micro scale, limiting their lifetime. To remove this restriction, many novel smart gels exhibit self-healing properties that restore their function and structure after damage. Hydrogels based on dynamic interactions have ability to self-heal after damage. The whole healing process does not require the induction of external stimuli (heat, light, pH or catalyst). The hydrogel exhibits excellent self-healing properties (Figure 4e,f). The entire self-healing process occurred in approximately 2 min. The self-healing process mainly benefits from the synergistic effect of multihydroxyl structures and dynamic covalent

bonds. The possible self-healing mechanisms are shown in Figure 4(g). First, the remaining -OH groups in PVA can rapidly form hydrogen bonds on the contact surface, but hydrogen bonds are weak and easily disrupted by mechanical deformation. Then, the anchoring of the free B(OH)_4^- on the PVA chains rapidly triggers of the self-healing process without external assistance.³⁹

In addition, to illustrate that addition of B(OH)_4^- increased the cross-linking density, a dynamic frequency sweep contrast experiment was performed on the hydrogels PVA/ C_nMPBr and PVA/ $\text{C}_n\text{MPBr}/\text{B(OH)}_4^-$. As shown in Figure S2, the storage modulus (G') is higher than the loss modulus (G'') for all hydrogel samples, which is indicative of the gel properties. For PVA/ C_nMPBr system, the addition of C_nMPBr to PVA solution causes a decrease in the modulus. Moreover, this change is more remarkable for a system with shorter carbon-chain C_nMPBr . ILS C_nMPBr with short chains are more hydrophilic than those with long chains. Therefore, long-chain ionic liquid molecules will aggregate to some extent in water due to hydrophilic-hydrophobic interactions, which results in larger moduli. After the addition of B(OH)_4^- , the cross-linked structure formed via the interaction between B(OH)_4^- and -OH groups of PVA, which results in the increased moduli.

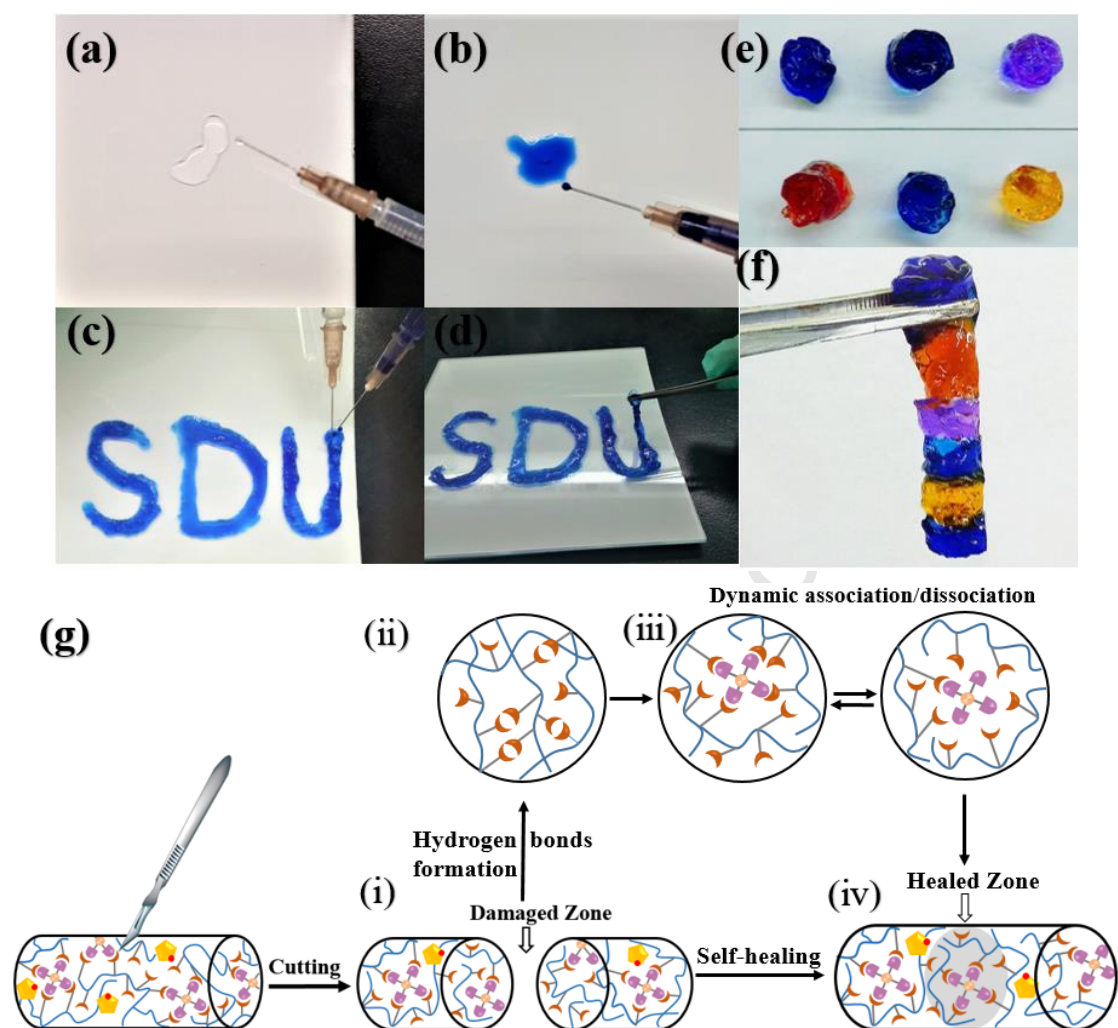


Figure 4. The gelation ability, injectability and self-healing of PVA/C₄MPBr/B(OH)₄⁻ hydrogels. (a) 0.5 mol/L mixed solution of C_nMPBr and B(OH)₄⁻; (b) 5 wt% pure PVA solution; (c) The two solutions are simultaneously pushed out from the syringes; (d) Hydrogel formation and self-support performance; (e) Several cylindrical hydrogel blocks dyed with different colors; (f) Self-supporting hydrogel was constructed by self-healing of small hydrogel blocks; (g) Schematic illustration of self-healing mechanisms of PVA/C_nMPBr/B(OH)₄⁻ hydrogels: (i) A cylindrical hydrogel is cut into two pieces using a knife.

(ii) The remaining -OH groups in PVA can rapidly form hydrogen bonds on the contact surface across the damaged zone. (iii) The dynamic association and dissociation of the borate ester bonds.

Water content and swelling of hydrogels are two important aspects that affect gel performance. High water content can maintain a moist environment, which is beneficial to wound healing, and large swelling degree promotes to the absorption of wound exudates and prevents secondary bacterial infection.⁴⁰ DS test results indicate that gels have high moisture content (as high as 94%). The 3D network structure of the hydrogel endows the gel mechanical strength so that it cannot be disintegrated after absorbing an excessive amount of water. The degree of swelling is dependent on the structure of the hydrogel and the interaction of the polymer with the permeate.⁴¹ Figure 5 shows the swelling kinetics of hydrogels. Because PVA is hydrophilic in nature, water molecules can be easily absorbed by PVA hydrogel. All hydrogels exhibit rapid swelling at the initial stage. Then, the swelling equilibrium was achieved in 12 h at room temperature (Figure 5a). The results indicated that swelling degree of PVA/C_nMPBr hydrogel increased as the carbon chain length of ILs increased (Figure 5b). However, when B(OH)₄⁻ is added to form a cross-linked structure, the equilibrium swelling degree of the hydrogel was remarkably reduced because the fact that the addition of B(OH)₄⁻ causes a greater degree of cross-linking and the hydrogel backbone

becomes denser. This structure maintains the good mechanical properties of the hydrogel after absorbing a large amount of water.

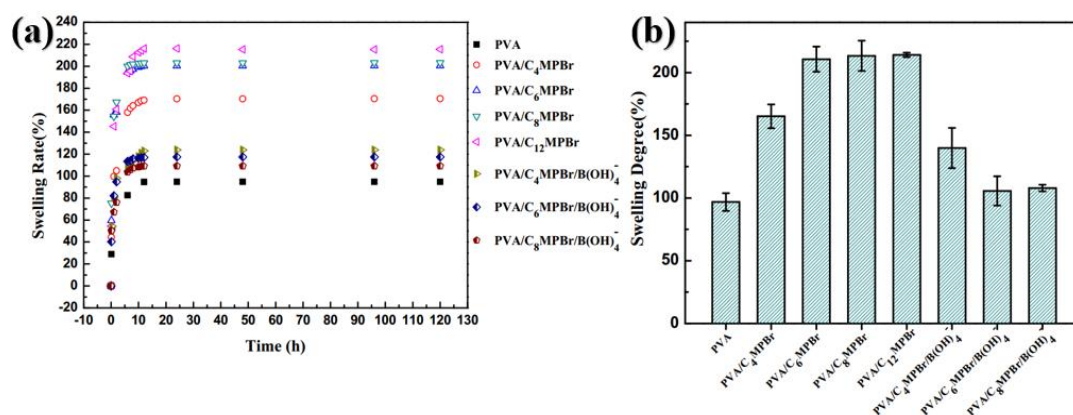


Figure 5. (a) Plot of swelling rate(%) versus time for different hydrogel samples; (b) swelling degree for different hydrogel samples.

The intriguing stimuli-responsive behavior of hydrogels has attracted widespread attention as biomimetic systems. Borate ester linkages have the ability to break and reform on exposure to certain environmental stimuli due to the reversible nature of dynamic covalent bonds.^{42, 43} The introduction of borate ester bond endows hydrogels with new functions, such as glucose responsivity and pH reversibility.⁴⁴ The rheological properties of PVA/B(OH)₄⁻ hydrogels have changed dramatically in the presence of glucose because the formed borate esters are dissociated in the presence of another competitive saccharide molecules, such as glucose.⁴⁵ Given their glucose responsivity, these hydrogels can be developed for glucose sensing or self-regulated insulin release.⁴⁴ Similarly, our investigated PVA/C₄MPBr/B(OH)₄⁻ system also exhibited an obvious glucose responsivity (Figure 6a). In addition, the

pH-responsive behavior of the hydrogels was also tested. As demonstrated in Figure 6b, given the highly pH-dependent and reversible binding between the boronic acid group and cis-diols, the PVA/C₄MPBr/B(OH)₄⁻ hydrogel showed pH-responsive features. The hydrogel underwent a gel-sol transformation process when the pH of the system was reduced by adding HCl. The significant change in rheological properties is attributed to the dissociation of borate ester bonds below the pK_a of the boronic acid component.⁴⁵⁻⁴⁹ In addition, this phase transition is reversible. When the pH was adjusted to the initial state by the addition of equimolar NaOH, the sample reverted back to a gel state. This reversible gel-sol conversion represents promising applications, especially for drug delivery in cancer targeting therapy.⁵⁰

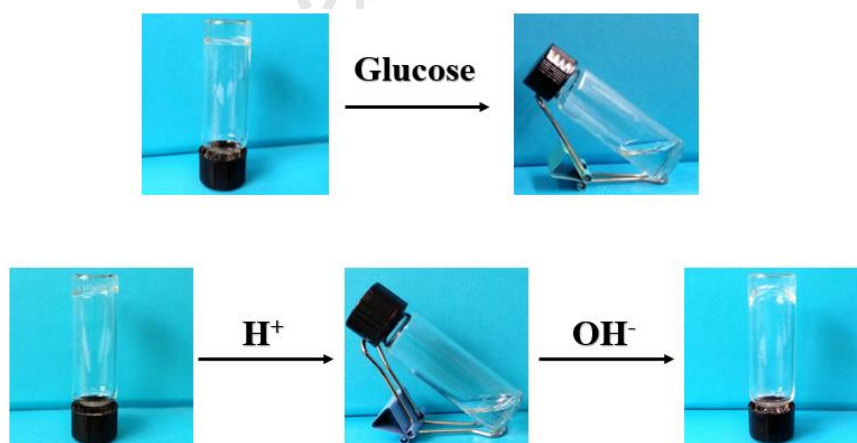


Figure 6. Glucose- and pH- responsive behaviors of PVA/C₄MPBr/B(OH)₄⁻ hydrogel.

To evaluate the antibacterial activity of ILs, microbiological assays were performed (Figure 7). In this study, the zone of inhibition test

method was used to examine the antibacterial activity of hydrogels. The inhibition zone averages for each bacterium are listed in Table S1. Without the addition of C_n MPBr, the pure PVA hydrogel displayed almost no antibacterial properties (Figure 7b,d). The clear inhibition zone was obvious after the incorporation of ILs. The superior antibacterial properties are mainly attributed to the bactericidal properties of ILs. It is worth noting that the carbon chain length of ILs is the most significant indicator of antimicrobial activity. We hypothesize that the role of ILs is similar to cationic liposomes, which can cause cell death through destruction of cell membrane.⁵¹ A schematic diagram of the possible bactericidal mechanism of ILs is presented in Figure 8. First, the ILs are preferentially adsorbed on the negatively charged cell membrane based on electrostatic interactions. Then, ILs with longer carbon chains tend to be inserted into the lipophilic region of the cell membrane, causing irreversible physical damage to weaken the bacterial resistance.²⁵ In addition, after the addition of borate ions, the inhibition zone becomes smaller. It is hypothesized that a cross-linked network structure was formed when $B(OH)_4^-$ was added. This structure facilitates the encapsulation of moisture and prevents the antibacterial ILs aqueous from diffusing easily, thereby achieving more efficient wound healing.⁵²

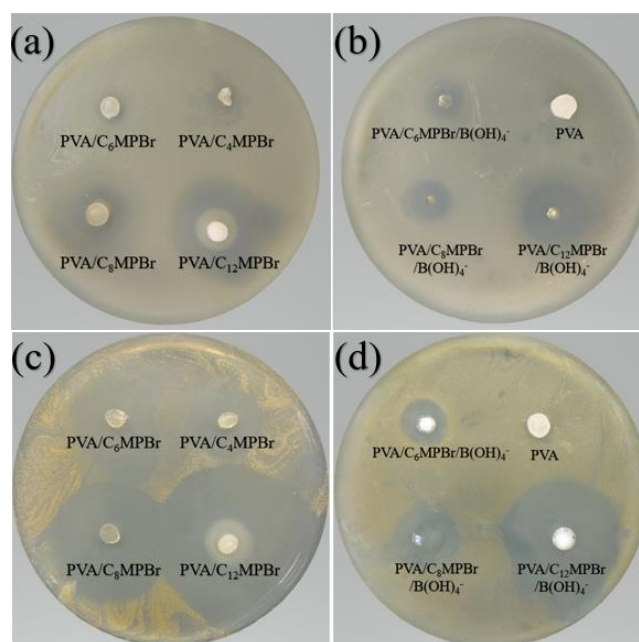


Figure 7. Inhibition zone against *Escherichia coli* (a)-(b) and *Staphylococcus aureus* (c)-(d) for pure PVA (prepared by freezing-thawing method), PVA/C_nMPBr and PVA/C_nMPBr/B(OH)₄⁻ hydrogels (n=4,6,8 and 12)

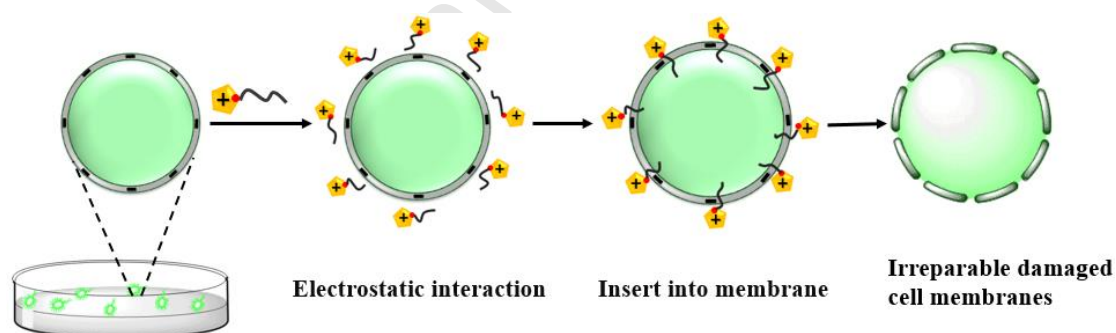


Figure 8. Schematic illustration of the possible bactericidal mechanism of ionic liquid (C_nMPBr).

Joints frequently move and bend. The ideal joint wound dressing makes good contact with the skin without hindering movement. Hydrogels composed of natural polymers with good tensile properties can be used to simulate the extensibility of human skin tissue.^{35, 53} The tensile properties

of PVA/C_nMPBr/B(OH)₄⁻ hydrogels were evaluated via tensile testing as shown in Figure S3-4. The hydrogels exhibited superior tensile properties (>200%) and maintained good ductility after healing. Furthermore, the hydrogels showed good adhesive properties on human knuckle skin (Figure S5). Therefore, these antimicrobial hydrogels have potential applications as dressing materials for joint skin wound healing.

Conclusion

In summary, we report a series of antibacterial hydrogels based on poly(vinyl alcohol) (PVA)-tetrahydroxyborate anion (B(OH)₄⁻) and pyrrolidinium ILs (C_nMPBr) for joint wound dressing. Poly(vinyl alcohol) (PVA)-B(OH)₄⁻ hydrogels were used as vectors and pyrrolidinium ILs (C_nMPBr) were used as antibacterial drugs. These antibacterial hydrogels exhibited multiple functions, including self-healing, syringeability and glucose and pH responsivity. Pyrrolidinium ILs (C_nMPBr) played a similar role to cationic liposomes that have been widely used as antibacterial drugs. The chemical structure of ILs and the hydrogel skeleton structure have an obvious effect on antibacterial properties. ILs with longer alkyl chain exhibited more pronounced antibacterial activities against *Escherichia coli* and *Staphylococcus aureus*, causing irreversible physical damage to weaken bacterial resistance. The three-dimensional (3D) network structure of hydrogels can prevent the leakage of antibacterial liquid, which is beneficial for accurate administration to the

wound area. The incorporation of borate linkages with dynamic cross-linking properties facilitates the responsiveness of the hydrogel. Furthermore, the hydrogels exhibit suitable stretchability and adhesive properties on human knuckle without any resistance, which indicating potential applications as dressing materials for joint skin wound healing.

Conflicts of interest

There are no conflicts to declare.

Acknowledgements

This work was supported by the National Natural Science Foundation of China (No. 21573132, No. 21773141).

References

1. M. Pooresmaeil and H. Namazi, *Polymers for Advanced Technologies*, 2019, **30**, 447-456.
2. S. Li, S. Dong, W. Xu, S. Tu, L. Yan, C. Zhao, J. Ding and X. Chen, *Adv Sci (Weinh)*, 2018, **5**, 1700527.
3. B. Balakrishnan, M. Mohanty, P. R. Umashankar and A. Jayakrishnan, *Biomaterials*, 2005, **26**, 6335-6342.
4. W. H. Eaglstein and MD, *Dermatol Surg*, 2001, **27**, 175-181.
5. C. Radhakumary, M. Antonty and K. Sreenivasan, *Carbohydrate Polymers*, 2011, **83**, 705-713.
6. X. Huang, Y. Zhang, X. Zhang, L. Xu, X. Chen and S. Wei, *Materials science & engineering. C, Materials for biological applications*, 2013, **33**, 4816-4824.
7. S. R. Caliri and J. A. Burdick, *Nature methods*, 2016, **13**, 405-414.
8. Q. Huang, Y. Zou, M. C. Arno, S. Chen, T. Wang, J. Gao, A. P. Doveand and J. Du, *Chem. Soc. Rev*, 2017, **46**, 6255-6275.
9. L. Liu, X. Feng, Y. Pei, J. Wang, J. Ding and L. Chen, *Materials science & engineering. C, Materials for biological applications*, 2018, **82**, 25-28.
10. J. C. Carrillo-Rodríguez, H. I. Meléndez-Ortiz, B. Puente-Urbina, G. Padrón, A. Ledezma and R. Betancourt-Galindo, *Polymer Composites*, 2018, **39**, 171-180.
11. B. V. Slaughter, S. S. Khurshid, O. Z. Fisher, A. Khademhosseini and N. A. Peppas, *Adv Mater*, 2009, **21**, 3307-3329.
12. T. Vermonden, R. Censi and W. E. Hennink, *Chemical reviews*, 2012, **112**, 2853-2888.
13. H. L. Lim, Y. Hwang, M. Kar and S. Varghese, *Biomater. Sci.*, 2014, **2**, 603-618.

14. B. Xue, V. Kozlovskaya and E. Kharlampieva, *J. Mater. Chem. B*, 2017, **5**, 9-35.
15. Z. Wei, J. H. Yang, J. Zhou, F. Xu, M. Zrinyi, P. H. Dussault, Y. Osada and Y. M. Chen, *Chemical Society reviews*, 2014, **43**, 8114-8131.
16. T. C. Tseng, L. Tao, F. Y. Hsieh, Y. Wei, I. M. Chiu and S. H. Hsu, *Adv Mater*, 2015, **27**, 3518-3524.
17. F. Karimi, J. Collins, D. E. Heath and L. A. Connal, *Bioconjugate chemistry*, 2017, **28**, 2235-2240.
18. J. Yan, G. Springsteen, S. Deeter and B. Wang, *Tetrahedron*, 2004, **60**, 11205-11209.
19. K. E. Boehle, J. Gilliland, C. R. Wheeldon, A. Holder, J. A. Adkins, B. J. Geiss, E. P. Ryan and C. S. Henry, *Angew Chem Int Ed Engl*, 2017, **56**, 6886-6890.
20. A. D. Miller, *Angew. Chem. Int. Ed.*, 1998, **37**, 1768-1785.
21. R. Kugler, O. Bouloussa and F. Rondelez, *Microbiology*, 2005, **151**, 1341-1348.
22. D. Coleman and N. Gathergood, *Chemical Society reviews*, 2010, **39**, 600-637.
23. M. Petkovic, K. R. Seddon, L. P. Rebelo and C. Silva Pereira, *Chemical Society reviews*, 2011, **40**, 1383-1403.
24. J. P. Hallett and T. Welton, *Chemical reviews*, 2011, **111**, 3508-3576.
25. C. Fang, L. Kong, Q. Ge, W. Zhang, X. Zhou, L. Zhang and X. Wang, *Polymer Chemistry*, 2019, **10**, 209-218.
26. M. Seter, M. J. Thomson, J. Stoimenovski, D. R. MacFarlane and M. Forsyth, *Chem Commun (Camb)*, 2012, **48**, 5983-5985.
27. J. Pernak and J. Feder-Kubis, *Chemistry - A European Journal*, 2005, **11**, 4441-4449.
28. S. Y. Choi, H. Rodríguez, A. Mirjafari, D. F. Gilpin, S. McGrath, K. R. Malcolm, M. M. Tunney, R. D. Rogers and T. McNally, *Green Chemistry*, 2011, **13**, 1527.
29. Z. Zheng, Q. Xu, J. Guo, J. Qin, H. Mao, B. Wang and F. Yan, *ACS applied materials & interfaces*, 2016, **8**, 12684-12692.
30. G. B. Thorat, S. Gupta and Z. V. P. Murthy, *Chinese Journal of Chemical Engineering*, 2017, **25**, 1402-1411.
31. A. Dixit, D. S. Bag, D. K. Sharma and N. Eswara Prasad, *Polymer International*, 2019, **68**, 503-515.
32. N. J. Bridges, K. E. Gutowski and R. D. Rogers, *Green Chem.*, 2007, **9**, 177-183.
33. N. R. Kubo, Y. James. T. D., *Chem. Commun.* , 2015, **51**, 2005-2020.
34. A. Dixit, D. S. Bag and S. J. S. Kalra, *Polymer*, 2017, **119**, 263-273.
35. J. Qu, X. Zhao, Y. Liang, T. Zhang, P. X. Ma and B. Guo, *Biomaterials*, 2018, **183**, 185-199.
36. D. Y. Ko, U. P. Shinde, B. Yeon and B. Jeong, *Progress in Polymer Science*, 2013, **38**, 672-701.
37. Y. Li, J. Rodrigues and H. Tomas, *Chemical Society reviews*, 2012, **41**, 2193-2221.
38. Y. Wu, L. Wang, B. Guo and P. X. Ma, *ACS nano*, 2017, **11**, 5646-5659.
39. G. Cai, J. Wang, K. Qian, J. Chen, S. Li and P. S. Lee, *Adv Sci (Weinh)*, 2017, **4**, 1600190.
40. K. Wang, J. Wang, L. Li, L. Xu, N. Feng, Y. Wang, X. Fei, J. Tian and Y. Li, *Chemical Engineering Journal*, 2019, **372**, 216-225.
41. P. J. Flory and J. Rehner., *J. Chem. Phys.* , 1943, **11**, 521-526.
42. L. Wang, M. Liu, C. Gao, L. Ma and D. Cui, *Reactive and Functional Polymers*, 2010, **70**, 159-167.
43. L. He, D. E. Fullenkamp, J. G. Rivera and P. B. Messersmith, *Chem Commun (Camb)*, 2011, **47**, 7497-7499.

44. Y. Guan and Y. Zhang, *Chemical Society reviews*, 2013, **42**, 8106-8121.
45. R. Guo, Q. Su, J. Zhang, A. Dong and C. Lin, *Biomacromolecules*, 2017, **18**, 1356-1364.
46. M. Nakahata, S. Mori, Y. Takashima, A. Hashidzume, H. Yamaguchi and A. Harada, *ACS Macro Letters*, 2014, **3**, 337-340.
47. M. Vatankhah-Varnoosfaderani, S. Hashmi, A. GhavamiNejad and F. J. Stadler, *Polym. Chem.*, 2014, **5**, 512-523.
48. F. Coumes, P. Woisel and D. Fournier, *Macromolecules*, 2016, **49**, 8925-8932.
49. H. Jia, X. Leng, Q. Wang, Y. Han, S. Wang, A. Ma, M. Guo, H. Yan and K. Lv, *Chemical Engineering Science*, 2019, **202**, 75-83.
50. M. A. M. a. S. J. R. R. J. Wojtecki, *Nat. Mater.*, 2011, **10**, 14-27.
51. S. B. K. Goel, M. Singh, D. Mondal, *RSC Adv*, 2016, **6**, 106806–106820.
52. C. W. Y. Zhou, Y. Yang, H. Yang, S. Wang, Z. Dai, K. Ji, H. Jiang, X. Chen, Y. Long, *Adv. Funct. Mater.*, 2019, **29**, 1806220.
53. N. Annabi, D. Rana, E. Shirzaei Sani, R. Portillo-Lara, J. L. Gifford, M. M. Fares, S. M. Mithieux and A. S. Weiss, *Biomaterials*, 2017, **139**, 229-243.

Conflicts of interest

There are no conflicts to declare.

Highlights:

1. The ILs as antibacterial drugs which exhibited antibacterial properties.
2. The hydrogel showed multifunction such as self-healing and multi-responsiveness.
3. The hydrogel can serve as dressing materials for joints skin wound healing.